Global-scale seismic interferometry: numerical validation of the acoustic correlation integral

Elmer Ruigrok, Deyan Draganov, Kees Wapenaar and Jan Thorbecke*
Delft University of Technology, Department of Geotechnology

Summary

Applying seismic reflection imaging on a global scale is hard due to the (locally) sparse source distribution. We approach this problem with seismic interferometry (SI). In this paper, we derive an expression for global-scale SI and test it on a simplified 2D acoustic lossless Earth model. When we use responses from sources placed all around the model, we can reconstruct the full and multiple-free response due to a simulated source at one of the receiver positions. When we miss the responses from near-offset sources, we can still reconstruct the full Green's function. We currently investigate which events in the Green's function we can still reconstruct properly when responses from sources in the mid- and far-offset range are missing.

Introduction

Seismic reflection imaging has shown its virtues on exploration scale, but has little been applied on a global scale due to the sparse source distribution; the earthquake hypocenters are mainly along the active lithospheric plate boundaries. This problem can be approached with Seismic Interferometry (SI).

In recent years there has been considerable progress in the development of SI techniques; for an overview see, e.g., Wapenaar et al. (2004), Schuster et al. (2004) and Campillo (2006). A source can be simulated at any receiver position by the application of a correlation integral. By measuring the responses of a medium at a receiver due to a number of sources and correlating these with the responses due to the same sources measured at other receivers and subsequently stacking the contributions of the different sources, the Green's function of the medium is reconstructed as if from a source at one of the receiver positions and receivers at the others.

The application of SI techniques on a global scale would simulate source locations at places where naturally no earthquakes occur. In this way, it would be possible to create a denser sampling of common-source gathers, improving the application of reflection imaging on a global scale.

In this paper, we derive a new correlation integral for global scale SI and verify it with numerical modeling.

Theory

Wapenaar and Fokkema (2006) derived relations for SI for exploration purposes starting with a reciprocity theorem of the correlation type. Here we follow their approach and start with the reciprocity relation in the frequency domain:

		State A: free surface	State B: no free surface
$wavefield$ $\mathbf{x} \in \mathbb{D}$	$\hat{P}_A$	$\hat{G}^{p,f}(\mathbf{x},\mathbf{x}_A,\omega)$	$\hat{G}^{p,q}_0(\mathbf{x},\mathbf{x}_B,\omega)$
	$\hat{V}_{i,A}$	$\hat{G}^{v,f}_i(\mathbf{x},\mathbf{x}_A,\omega)$	$\hat{G}^{v,q}_{0,i}(\mathbf{x},\mathbf{x}_B,\omega)$
$wavefield$ $\mathbf{x} \in \partial\mathbb{D}$	$\hat{P}_A$	$\delta(\mathbf{x}-\mathbf{x}_A)$	$\hat{G}^{p,q}_0(\mathbf{x},\mathbf{x}_B,\omega)$
	$\hat{V}_{i,A}$	$\hat{G}^{v,f}_i(\mathbf{x},\mathbf{x}_A,\omega)$	$\hat{G}^{v,q}_{0,i}(\mathbf{x},\mathbf{x}_B,\omega)$
$source$ $\mathbf{x}_B \in \mathbb{D}$	$\hat{Q}_A$	0	$\delta(\mathbf{x}-\mathbf{x}_B)$
	$\hat{F}_{i,A}$	0	0

Table 1: States for the acoustic reciprocity theorem.

$$\oint_{\partial\mathbb{D}} (\hat{P}^*_A \hat{V}_{i,B} + \hat{V}^*_{i,A}\hat{P}_B)\mathbf{n}d^2\mathbf{x} = \int_{\mathbb{D}} (\hat{P}^*_A \hat{Q}_B + \hat{V}^*_{i,A}\hat{F}_{i,B} + \hat{F}^*_{i,A}\hat{V}_{i,B} + Q^*_A P_B)\mathbf{n}d^2\mathbf{x}. \quad (1)$$

In equation 1, $\hat{P}$ and $\hat{V}_i$ denote the pressure and particle velocity (the hat above the symbols denote that they are in the frequency domain; $_i$ stands for the components of a vector in space); $\hat{Q}$ and $\hat{F}_i$ are the volume injection rate and force sources; A and B stand for two acoustic states in one and the same domain; $\mathbb{D}$ stands for a domain containing a lossless inhomogeneous acoustic medium, enclosed by a surface $\partial\mathbb{D}$.

The representation for state A and state B that we use in this paper are listed in Table 1. The first and second superscript of the Green's function $\hat{G}$ denote, respectively, the observed response type (p - pressure; v - particle velocity) and the source type (f - force; q - injection rate). The subscripts $_0$ denotes response without free-surface multiples and $_i$ denotes the direction in which the observed quantity is measured. $\hat{G}(\mathbf{x},\mathbf{x}_A,\omega)$ is the response of the medium observed at $\mathbf{x}$, due to a source in $\mathbf{x}_A$. State A is an approximate physical representation of an earthquake occurring in the Earth. State B is a representation of an earthquake occurring in an Earth without free surface. State B can be extracted out of State A using, e.g., surface related multiple elimination, see Berkhout and Verschuur (1997) and Verschuur and Berkhout (1997). $\partial\mathbb{D}$ is taken just below the free surface. In state A, we choose a delta function as a directional source f located on the Earth's surface (the free surface), see Figure 1a. In state B, we choose an omnidirectional source q just within the domain $\mathbb{D}$, see Figure 1b. The wavefields are registered at $\partial\mathbb{D}$. Substituting the representation (Table 1) in equa-

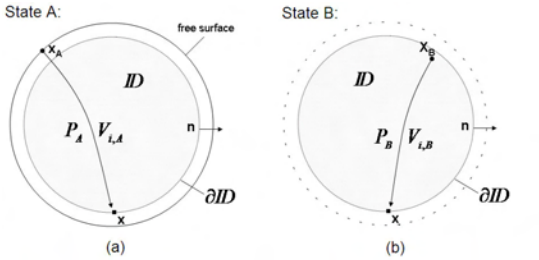

Fig. 1: Location of $\mathbf{x}_A$, $\mathbf{x}_B$ and $\mathbf{x}$ on the simplified 2D acoustic Earth model. Starting just below the Earth's surface, a domain $\mathbb{D}$, enclosed by the surface $\partial\mathbb{D}$, covers the whole inner space of the Earth. P and V_i describe the wavefields within $\mathbb{D}$ and on $\partial\mathbb{D}$ due to a source in $\mathbf{x}_A$ or $\mathbf{x}_B$. (a) State A, Earth with free surface; $x_{i,A}$ lays just outside $\mathbb{D}$, on the free surface. (b) State B, Earth without free surface; $\mathbf{x}_B$ lays just within $\mathbb{D}$.

tion 1 and making use of the sifting property of the delta function yields

$$\oint_{\partial\mathbb{D}} \{\hat{G}^{v_r,f}(\mathbf{x},\mathbf{x}_A,\omega)\}^* \hat{G}_0^{p,q}(\mathbf{x},\mathbf{x}_B,\omega)d^2\mathbf{x} = \hat{G}^{p,f}(\mathbf{x}_B,\mathbf{x}_A,\omega)^* - \hat{G}_0^{v_r,q}(\mathbf{x}_A,\mathbf{x}_B,\omega). \quad (2)$$

In equation 2 only the radial direction of the particle velocity, denoted by v_r, remains by the vector multiplication between G_i^v and $\mathbf{n}$. Applying source-receiver reciprocity and the inverse Fourier transform, gives the expression in the time domain:

$$\oint_{\partial\mathbb{D}} G^{v_r,f}(\mathbf{x}_A,\mathbf{x},-t) * G_0^{p,q}(\mathbf{x}_B,\mathbf{x},t)d^2\mathbf{x} = G^{p,f}(\mathbf{x}_B,\mathbf{x}_A,-t) + G_0^{p,f}(\mathbf{x}_B,\mathbf{x}_A,t). \quad (3)$$

Equation 3 is the global-scale SI relation.

Modeling

Relation 3 is numerically tested on a simplified 2D acoustic lossless Earth model based on the Preliminary Reference Earth Model, see Dziewonski and Anderson (1981). The medium parameters vary only in the radial direction (r), see Figure 2.

In state A, an omnidirectional source is placed just below the free surface. The interference between the direct and free-surface-reflected wavefield gives effectively a directional source located at the free surface. As a source we use the first derivative of a Gaussian wavelet.

The resulting wavefield is modeled with a staggered finite-difference scheme of the acoustic wave equation. p and v_r are registered at a position just below the Earth's surface. Figure 5 shows the Earth's response measured at 0° epicentral distance, due to sources all around the model, for (a) state A and (b) state B. These are the radial particle velocity and pressure Green's functions convolved with a source wavelet.

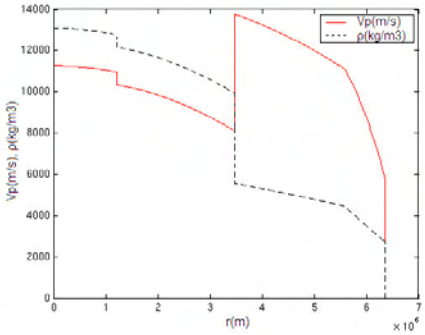

Fig. 2: The smoothed version of PREM. The P-wave velocity V_p and density ρ are depicted as functions of the radius r. The radius is chosen to be zero at the center of the Earth. With increasing r, subsequently the inner core-outer core boundary, the outer core-mantle boundary and the crust-atmosphere boundary (free surface) are encountered. The discontinuities in the upper mantle and crust are not considered in this model.

Numerical verification

After having modeled $G^{v_r,f}(\mathbf{x}_A,\mathbf{x},t)$ and $G_0^{p,q}(\mathbf{x}_B,\mathbf{x},t)$, we test the correlation integral, equation 3. The first step is a crosscorrelation between the anti-causal v_r-response with free-surface multiples measured at $\mathbf{x}_A$, with the multiple-free p-response measured at $\mathbf{x}_B$. The result is an intercorrelation gather, as visualized in Figure 3. The different traces correspond to different sources. The second step is depicted in Figure 4. It is an integration over all the sources, which comes down to a stacking of all the traces in the intercorrelation gather. As explained by Wapenaar et al. (2004), events around stationary phases should add up to simulate physical events and all the other energy should cancel. The resulting single trace has a causal as well as an anti-causal part. According to equation 3, the anti-causal part should be the p-response at $\mathbf{x}_B$ as if from a source at $\mathbf{x}_A$. The causal part should be the corresponding multiple-free p-response.

Steps 1 and 2 are repeated for all $\mathbf{x}_B$'s around the model. The first 3000 seconds of the result are depicted in Figures 6a and 6b. The input for the correlation integral had a modeling time of 6000 seconds. Comparing Figure 6 with Figure 5, it can be seen that indeed we have reconstructed the full and multiple-free Green's function, measured at all epicentral distances, due to a simulated source at $\mathbf{x}_A$. Figure 6b looks more noisy due to correlation artifacts.

Towards application

In reality one would like to simulate a source on a place where no earthquakes occur. This would be identical with at least missing the zero and near-offset traces of the common-receiver gather. In Table 1 the pressure response has been represented as a delta pulse. But when the locations at/near the source are missing, the pressure response detected at/near the free surface approximates

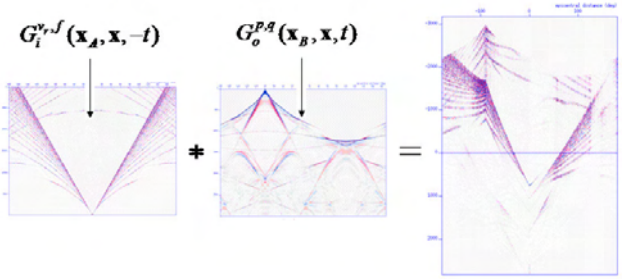

Fig. 3: Visualization of the integrand of equation 3. The left panel depicts the time reversed response of state A recorded at 0° epicentral distance. It is correlated with the response of State B recorded at −90° epicentral distance (middle panel). The right panel shows the resulting intercorrelation gather.

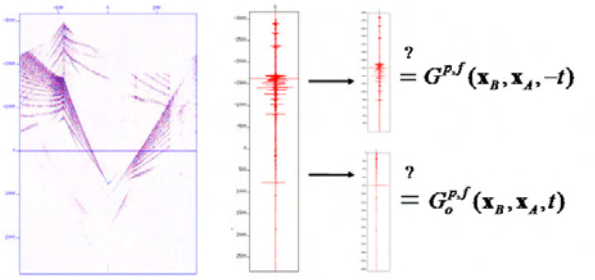

Fig. 4: Visualization of the integration process. The traces in the intercorrelation gather (left) are summed to produce the trace in the middle panel. The causal and anti-causal part are depicted separately.

zero. Replacing $\hat{P}_A = \delta(\mathbf{x}-\mathbf{x}_A)$ at $\mathbf{x} \in \partial\mathbb{D}$ with $\hat{P}_A = 0$ in Table 1 and repeating the derivation as has been made in the theory part, we obtain

$$\oint_{\partial\mathbb{D}} G^{v_r,f}(\mathbf{x}_A,\mathbf{x},-t) * G_0^{p,q}(\mathbf{x}_B,\mathbf{x},t)d^2\mathbf{x} = G^{p,f}(\mathbf{x}_B,\mathbf{x}_A,-t). \quad (4)$$

Equation 4 states that we can only reconstruct the response including the free-surface multiples, when no measurements of near sources are available.

We repeat the numerical validation, as described in the previous section, but now without using the near-offset traces in the modeled responses. Figure 7a shows the result. It was produced using 2880 sources around the model. Comparing it with Figure 5 we see that the Green's function is correctly reconstructed and the correlation noise is canceled out almost perfectly. Contrary to this, when using only 1440 sources around the model a lot of correlation noise is left, as can be seen on Figure 7b.

Discussion and Conclusions

In the previous section, we showed what happens if we do not have measurements in the near offset. In reality, we will not have a dense (earthquake) source distribution in some mid- and far-offsets either. As can be shown with stationary phase analysis, having dense source distribution only at certain epicentral distances, will reconstruct correctly only specific events in the Green's function. This is currently under investigation.

The representation used here, see Table 1 and Figure 1, is only valid for sources and receivers positioned all within one wavelength from the free surface. When this is not the case we may have to revise the representation and derivation. Additionally, in reality we have an elastic 3D Earth with many extra complexities. Also these extensions are currently under investigation.

In conclusion, we derived an acoustic correlation integral for global-scale SI and verified it with numerical modeling results. When responses from sources all over the simplified Earth model are available, then the correlation integral reconstructs the Earth's Green's function from a simulated source. When no near-offset sources are being used in the integration process, we can still reconstruct the Green's function with free surface multiples as long as the sampling of real source locations is dense enough.

Acknowledgments

This research is supported by The Netherlands Research Centre for Integrated Solid Earth Sciences ISES. The authors would like to thank Dirk Kraaijpoel and Xander Campman for helpful discussions on SI and Eric Verschuur for support in implementing SRME.

References

Berkhout, A. J. and D. J. Verschuur, 1997, Estimation of multiple scattering by iterative inversion, part i: Theoretical considerations: Geophysics, **62**, 1586–1595.

Campillo, M., 2006, Phase and correlation in 'random' seismic fields and the reconstruction of the green function: Pure and Applied Geophysics, **163**, 475–502.

Dziewonski, M. and D. L. Anderson, 1981, Preliminary reference earth model: Physics of The Earth and Planetary Interiors, **25**, 297–356.

Schuster, G. T., J. Yu, J. Sheng, and J. Rickett, 2004, Interferometric/daylight seismic imaging: Geophysical Journal International, **157**, 838–852.

Verschuur, D. J. and A. J. Berkhout, 1997, Estimation of multiple scattering by iterative inversion, part ii: Practical aspects and examples: Geophysics, **62**, 1596–1611.

Wapenaar, C. P. A., D. Draganov, J. van d̃er Neut, and J. W. Thorbecke, 2004, Seismic interferometry: a comparison of approaches: 74th Annual International Meeting, SEG, 1981–1984.

Wapenaar, C. P. A. and J. Fokkema, 2006, Green's functions representations for seismic interferometry: Geophysics, **in press**.

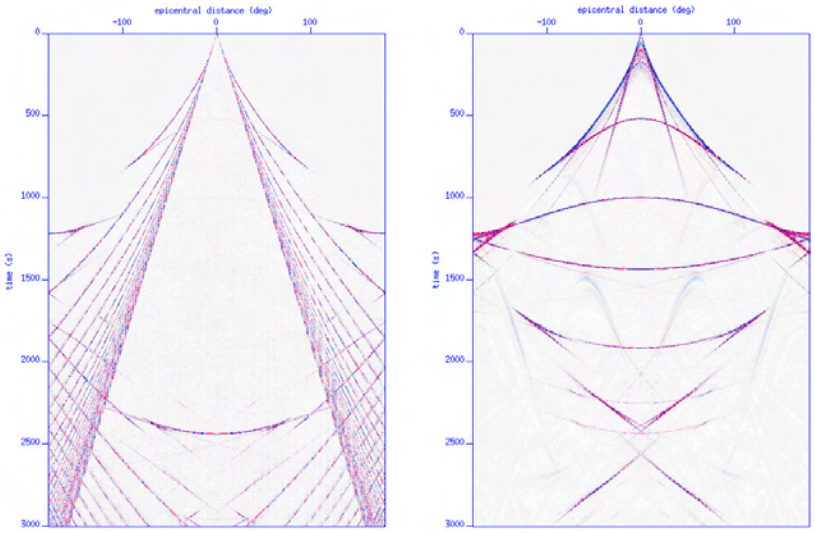

Fig. 5: The modeled reflection responses of the Earth. The horizontal axis shows epicentral distance in degrees and the vertical axis shows time in seconds; (a) state A, the modeled p-response including surface multiples; (b) state B, the modeled v_r-response, without the free-surface multiples.

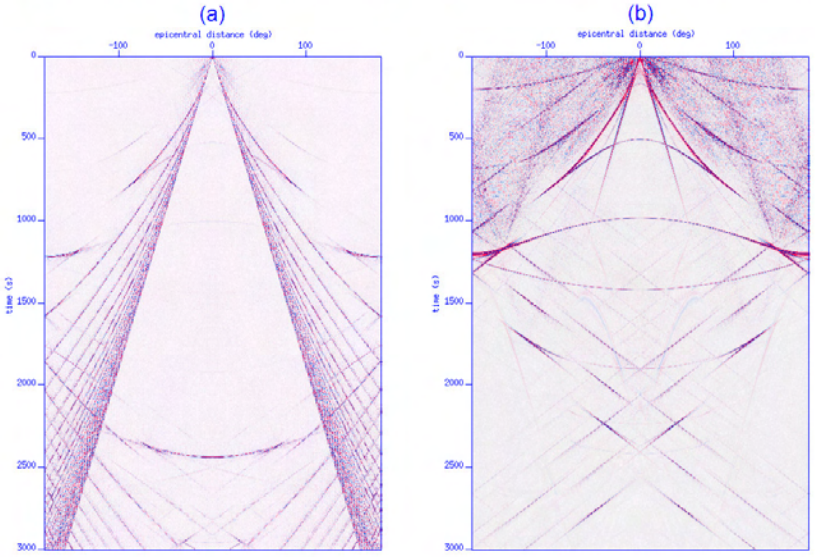

Fig. 6: The result of the numerical verification, using equation 3, for a simulated source ($\mathbf{x}_A$) at 0° epicentral distance and receivers ($\mathbf{x}_B$) at all epicentral distances. The horizontal axis shows epicentral distance in degrees and the vertical axis shows time in seconds; (a) the time-reversed anti-causal result; (b) the causal result.

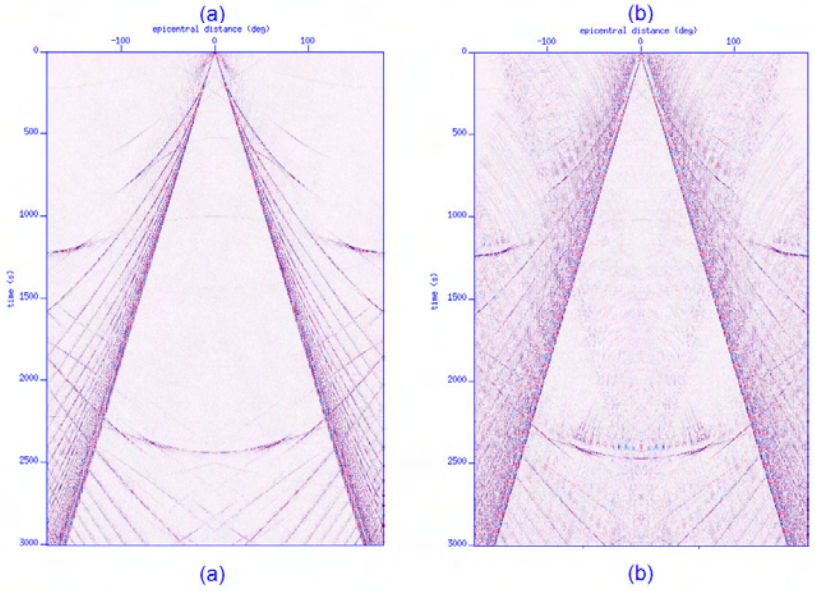

Fig. 7: The result of the numerical verification, using equation 4, for a simulated source ($\mathbf{x}_A$) at 0° epicentral distance and receivers ($\mathbf{x}_B$) at all epicentral distances. The horizontal axis shows epicentral distance in degrees and the vertical axis shows time in seconds; (a) the time-reversed anti-causal result using 2880 sources; (b) the time-reversed anti-causal result using 1440 sources.

EDITED REFERENCES

Note: This reference list is a copy-edited version of the reference list submitted by the author. Reference lists for the 2006 SEG Technical Program Expanded Abstracts have been copy edited so that references provided with the online metadata for each paper will achieve a high degree of linking to cited sources that appear on the Web.

REFERENCES

Berkhout, A. J., and D. J. Verschuur, 1997, Estimation of multiple scattering by iterative inversion, part I: Theoretical considerations: Geophysics, **62**, 1586–1595.

Campillo, M., 2006, Phase and correlation in random seismic fields and the reconstruction of the green function: Pure and Applied Geophysics, **163**, 475–502.

Dziewonski, M., and D. L. Anderson, 1981, Preliminary reference earth model: Physics of The Earth and Planetary Interiors, **25**, 297–356.

Schuster, G. T., J. Yu, J. Sheng, and J. Rickett, 2004, Interferometric/daylight seismic imaging: Geophysical Journal International, **157**, 838–852.

Verschuur, D. J., and A. J. Berkhout, 1997, Estimation of multiple scattering by iterative inversion, part II: Practical aspects and examples: Geophysics, **62**, 1596–1611.

Wapenaar, C. P. A., D. Draganov, J. van der Neut, and J. W. Thorbecke, 2004, Seismic interferometry: a comparison of approaches: 74th Annual International Meeting, SEG, Expanded Abstracts, 1981–1984.

Wapenaar, C. P. A., and J. Fokkema, 2006, Green's functions representations for seismic interferometry: Geophysics, in press.